J Mater Sci (2010) 45:1993–2001
DOI 10.1007/s10853-009-4061-z

HTC2009

Surface tension of γ-TiAl-based alloys

R. Nowak · T. Lanata · N. Sobczak ·
E. Ricci · D. Giuranno · R. Novakovic ·
D. Holland-Moritz · I. Egry

Received: 12 June 2009 / Accepted: 21 November 2009 / Published online: 10 December 2009

Abstract Within the Integrated Project IMPRESS, funded by the EU, a concerted action was taken to determine the thermophysical properties of a γ-TiAl-based alloys, suitable for casting of large turbine blades for aero-engines and stationary gas turbines. The challenge was to develop a castable alloy, free of grain refiners and susceptible to heat treatment. Owing to the high reactivity of this class of alloys, many difficulties were encountered to process the liquid phase in a crucible. This prevented also the measurements of specific heat, viscosity and electrical conductivity in the liquid phase. However, surface tension and density could be measured using container-less techniques. For the surface tension determination, both the oscillating droplet method by the electromagnetic levitation as well as a combined method using two methodologies in one test (i.e. the pendant drop and sessile drop) by an advanced experimental complex that has been designed for investigations of high temperature capillarity phenomena were applied. All the quantities have been obtained as a function of temperature, in some cases also in the undercooled liquid. In this article, we report a comparative discussion on the results obtained for the surface tension of Ti–Al–Nb and Ti–Al–Ta alloys, together with the corresponding theoretical values calculated by thermodynamic models.

Introduction

Owing to a set of favourable properties, such as a low density, high melting temperature, good elevated-temperature strength, high resistance to oxidation and excellent creep properties, the TiAl-based intermetallics alloys are considered as having a high potential as structural materials for various applications in the gas turbine and automotive industry [1].

Within the Intermetallic Materials Processing in Relation to Earth and Space Solidification Project [2] (IMPRESS), selected by the European Commission as an Integrated Projected in its 6th Framework, the advancement of γ-TiAl alloys for 40 cm cast turbine blades for aero-engines and stationary gas turbines was aimed. Generally speaking, the IMPRESS Project's main objective is a better understanding of the links between materials processing routes, structure and final properties of a set of selected intermetallic alloys such as the γ-TiAl alloys as well as the NiAl alloys, these last for <20 µm-sized catalytic powder for use in hydrogen fuel cell electrodes and hydrogenation reactions. In the framework of the project, the whole production chain was analysed by numerical modelling: from alloy design based on the updated calculations of the phase diagrams, casting and microstructure evolution simulation for γ-TiAl alloys or simulation of the gas atomization process in the case of

---

R. Nowak · N. Sobczak
Foundry Research Institute (CHTS), 73 Zakopianska Street,
30-418 Cracow, Poland

T. Lanata
DICAT Dept., University of Genoa, via Opera Pia 15,
Genoa, Italy

E. Ricci (✉) · D. Giuranno · R. Novakovic
Inst. for Energetics and Interphases (CNR-IENI), Via de Marini
6, 16149 Genoa, Italy
e-mail: e.ricci@ge.ieni.cnr.it

D. Holland-Moritz · I. Egry
German Aerospace Center (DLR), 51170 Cologne, Germany

NiAl alloys. For such modelling, to produce realistic results, the reliable and accurate thermophysical properties data are needed. Thus, the measurement of thermophysical properties plays a key role, linking the experimental work and the modelling. The surface tension data are particularly relevant as the input data for the casting and solidification models.

Moreover, as for the investment casting process, the choice of mould/crucible material is also a critical issue for the measurements of thermophysical properties. High solidification temperature and chemical melt reactivity both request thermo-stable and chemically inert materials for crucibles/containers.

In fact, one of the main problems concerning the reproducibility of property data of alloys being solidified is related with contamination of melts, particularly by oxygen coming from the surrounding atmosphere, or from melt/crucible interactions.

In particular, it is well known that for TiAl-based melts, no chemically inert refractory materials can be found [3]. Such information is of a great interest not only for the purpose of fundamental solidification studies or for induction melting of TiAl-based alloys in ceramic crucibles and their investment casting into ceramic moulds but also for reliable measurements of the fundamental properties of these alloys. This is the main reason why container-less methods were used in majority for both, recent fundamental directional solidification studies [4] and thermophysical properties measurements [5].

Since further improvement of materials properties of TiAl alloys can be achieved by alloying (e.g. oxidation resistance may be improved by alloying with niobium or tantalum [6, 7]), two ternary Ti–Al–X (X = Nb, Ta) alloys were chosen, which are the subject of the surface tension measurements reported here. Their nominal composition is $Al_{45.5}Ti_{46.5}Nb_8$ and $Al_{45.5}Ti_{46.5}Ta_8$ (in at%).

In order to discern potential sources of systematic measurement errors associated with different equipments and/or methods and to improve the reliability of the surface tension data, the measurements have been performed in parallel by different laboratories, applying the containerless Oscillating Droplet method by the Electro-Magnetic Levitation [8] and a new application at high temperature of the pendant/sessile drop (PD/SD) combined method. The related problems concerning the interactions with crucible/capillary ceramic materials have been also discussed.

The results have been compared with the calculated values obtained by applying theoretical modelling (e.g. Compound Formation Model-CFM and Quasi Chemical Approximation for Regular Solution-QCA for RS) for better understanding of the factors influencing the compositional dependence of the surface tension and to provide a proper interpretation of the experimental results.

Materials and methods

Samples of plasma melted $Al_{46}Ti_{46}Nb_8$ and $Al_{46}Ti_{46}Ta_8$ alloys, rod shaped, were supplied by the courtesy of ACCESS Company. The SEM/EDS analyses performed on the as-received samples revealed a homogeneous structure for the Nb-containing alloy, whilst the Ta-containing alloy showed the presence of W traces and some Ta precipitates (Fig. 1).

Before the surface tension measurements by the pendant/sessile drop combined method, the rod of each ternary alloy was cut into samples of desired weight (average weight value = 10 g), mechanically abraded and ultrasonically rinsed in ethanol. In order to preserve the original composition and microstructure, the pre-melting of alloys was not carried out. A high dense alumina (99.7%) plate ($\phi = 17.015$ mm) coated by the Y_2O_3 spray of chemical composition given by producer (ZYP Coatings Inc., USA) as Y_2O_3 98%, MgO 0.7% and SiO_2 1.3%, has been used for the sessile drop measurements, due to its improved chemical stability as a consequence of the formation of a stable Y–Al–O type ternary oxide [9, 10]. After covering with Y_2O_3 spray, the alumina parts (substrates, crucibles) were dried in air for 1 h and then heat-treated in two stages:

(I) $T_{max} = 1373$ K (3 h), $dT/dt = 3$ K/min, air
(II) $T_{max} = 1773$ K (1 h), $dT/dt = 5$ K/min, flowing pure Argon

Similar procedures were applied to the alloy samples used for the alloy/ceramic substrates interaction tests. In such case, the average weight value of the samples was about 0.2 g, and the plates of different ceramic materials were used as substrates having dimensions: $h = 3$ mm, $\phi = 14$ mm.

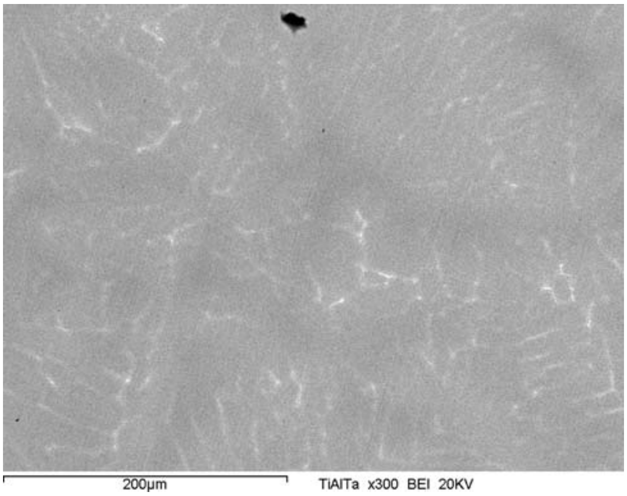

Fig. 1 SEM micrograph of as-received specimen of $Al_{46}Ti_{46}Ta_8$ alloy (white spots: Ta precipitates)

For the EML-OD experiments, the samples were prepared in the same way as for the sessile drop. The sample weight in this case was about 1 g.

Surface tension measurements by the oscillating drop method

The surface tension of stable and undercooled $Al_{46}Ti_{46}Nb_8$ and $Al_{46}Ti_{46}Ta_8$ melts were measured by use of the electromagnetic levitation device as described in [8]. For determination of the surface tension, the oscillating droplet method was applied. The oscillations of the sample surface are recorded from the top of the levitator with a video camera at a frame rate of 400 Hz with a pixel resolution of 1024 × 1000 pixels. At each investigated temperature, a series of 4096 frames is acquired. From the video sequences, frequency spectra of the sample radius, R, are determined. The spectrum contains five peaks at the frequencies ω_i ($i = -2, -1, 0, 1, 2$) resulting from the surface oscillations. Moreover, three translational frequencies T_x, T_y and T_z can be identified. From the five surface oscillation frequencies and the three translational frequencies, the surface tension, γ, is determined using the formula by Cummings and Blackburn [11]:

$$\gamma = \frac{3M}{160\pi} \sum_{m=-2}^{2} \varpi_i^2 - 1.9 \cdot \Omega^2 - 0.3 \cdot \left(\frac{g}{a}\right)^2 \Omega^{-2} \qquad (1)$$

with

$$\Omega^2 = \frac{1}{3}\left(T_x^2 + T_y^2 + T_z^2\right) \qquad (2)$$

Here, M denotes the sample mass.

Surface tension measurements by the pendant/sessile drop combined method

Owing to the high value of melting temperatures and the presence of high reactive elements, such as Ti, it was foreseen a very low possibility to perform measurements of surface tension of the Al–Ti-based alloys by applying the conventional methods, such as the sessile or the large drop methods [12]. However, an attempt has been done, by applying a combined method using two methods in one test (i.e. the pendant drop and sessile drop methods) by an advanced experimental complex that has been designed for investigations of high temperature capillarity phenomena (up to 2400 K) and described in details in [13].

The main part of the complex is high temperature chamber working under UHV or flowing inert gas and equipped with

(1) Heating system (Ta heater, Ta and Mo isolation screens, four thermocouples located in different positions in the furnace, computer programmed power transformer);
(2) Quadrupole residual gas analyzer with real-time recording for characterization of gaseous reaction products and gases formed during materials heating;
(3) Devices for keeping static or flowing gas with controlled rate at required level of pressure, experimental table (support made from alumina or Ta);
(4) A set of manipulators of special design allowing (a) to bring the samples of different sizes and various shapes between the chambers; (b) to change the position the heater and isolation screens by their up-and-down movement; (c) to change the position of experimental table by its rotation, and up-and-down or XY plane movement; (d) to change the position of thermocouples, one of them can be rotated or moved up and down to check the temperature field inside the testing area; (e) to introduce from the top of the chamber an additional substrate (transferred drop procedure) or capillary with a testing metal (dispensed drop procedure coupled with capillary purification to clean the drop surface from its primary oxide film), both with up-and-down movement options; and
(5) High-resolution digital camera with a system for real-time recording of sample images during high temperature studies.

Schematic illustration for positioning of samples (metal and substrate) and thermocouples is shown in Fig. 2. For pendant drop method, the metal is placed in alumina capillary (external diameter = 4.1065 mm), melted and after reaching of required temperature, squeezed through a hole in the capillary (hole diameter = 1.1 mm). The drop images are recorded by high-speed digital camera (1000 flames/s). After a few seconds, the droplet was put in contact with the substrate (by moving the capillary down and the substrate up) kept a few seconds and next, the droplet has been extended and broken (by moving the capillary and the substrate in the reverse directions) to deposit a sessile drop resting on the substrate.

This methodology was never applied before to measure the surface tension of high melting metal systems, except for the measurements on a set of refractory elements by simple pendant drop method as described in [14]. However, the procedures of the drop formation applied in this study and based on the use of a dispensed capillary device, as well as the procedure for the determination of the surface tension values based on the acquisition and elaboration of the pendant drop profile, differ substantially from the procedures and the analysis described in [14].

Despite the fact that in the proposed procedure the contact of a liquid metal with either a capillary or a

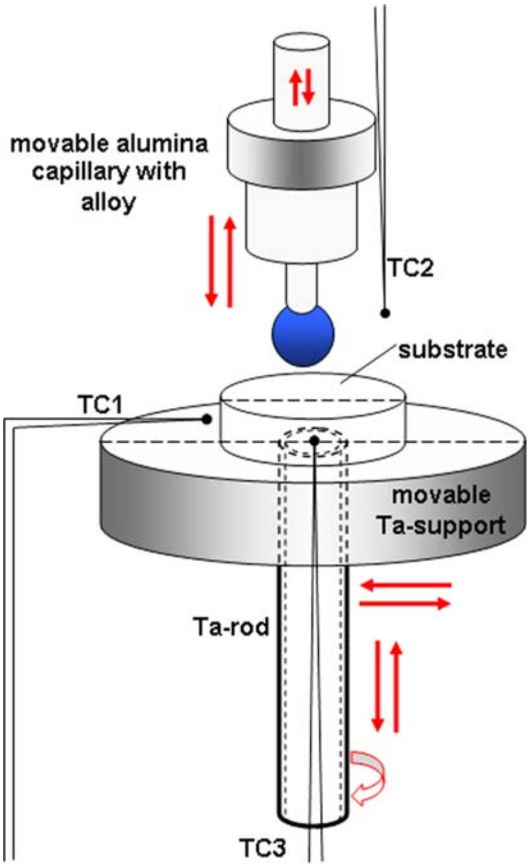

Fig. 2 Schematic presentation of positioning of testing samples and thermocouples during surface tension measurements by a combined pendant drop/sessile drop method

substrate is unavoidable, it assures essential advantages such as (1) this contact is very short (a few seconds), compared to conventional sessile drop procedure, (2) similar to a large drop method, the droplet deposited on a substrate has a high symmetry achieved by extending of a liquid, as experimentally confirmed by the rotation of the support, (3) contrary to simple pendant drop test, the droplet squeezed through capillary is free of primary oxide film that is particularly important for investigation of oxidizable alloys, as those of this study and (4) importantly, the same oxide film plays a role of barrier that might reduce or even prevent the interaction of the metal with the capillary during heating.

Interaction/wetting tests

A special challenge, in high temperature thermophysical property measurements, i.e. surface tension, is represented by the intrinsic reactivity of all the materials with the containers, particularly pronounced for Al-based and Ti-based alloys. This means, as can be shown on the basis of thermodynamic arguments, that the surface tension values obtained in many experiments do not really refer to pure substances, but rather to alloys or solutions, especially taking into account certain surface active elements and reaction products that have a drastic effect on the surface tension even if present in traces.

Interaction tests between the $Al_{46}Ti_{46}X_8$ (X = Nb, Ta) alloy and different 'common' ceramic substrates (Sapphire, dense Alumina, Zirconia) at the alloy melting temperature have been performed by the sessile drop method with the aim to find the most suitable crucible material, and thus to address correctly surface tension measurements. The following ceramic materials were used:

(1) Dense PolyCrystalline (PC) alumina (99.99% Al_2O_3) substrates produced by high-temperature sintering,
(2) Single Crystal (SC) Al_2O_3 (sapphire) of ~ 2 nm roughness,
(3) Polycrystalline ZrO_2 (YSZ) produced by high-temperature sintering,
(4) Novel polycrystalline ZrO_2 substrates produced by high-temperature sintering using addition of Y_2O_3 nanoparticles that was demonstrated recently to be effective for reduction of reactivity of high temperature Ni-and Ti-based alloys, compared to conventional YSZ.
(5) The wetting experiments have been carried out under a flowing pure Argon (99.9999%, $[O_2] < 0.1$ ppm; ArN60-Air Liquide) atmosphere using contact heating of the alloy/ceramic couples. The oxygen content in the surrounding atmosphere is further reduced due to the presence of Ta as heating element ($P_{O_2} < 10^{-9}$ Pa at $T = 1903$ K) [13]. The furnace temperature has been increased up to melting of the alloy sample.

Both $Al_{46}Ti_{46}Nb_8$ and $Al_{46}Ti_{46}Ta_8$ alloys exhibit reactive wetting behaviour towards the aforementioned ceramic materials. When the liquid phase is obtained, the contact angle rapidly decreases to a value of $\vartheta \leq 55°$, as shown in the case of the couple $Al_{46}Ti_{46}Ta_8$/Sapphire.

The SEM/EDS analyses of the cross-sections of both $Al_{46}Ti_{46}Nb_8$/alumina (SC, PC) and $Al_{46}Ti_{46}Ta_8$/(PC and YSZ) samples were performed. Both the alloys in contact with alumina have shown diffusion of the substrate material inside the metal bulk without formation of reaction layer, whilst the analysis of the $Al_{46}Ti_{46}Ta_8$/YSZ interface showed a thick reaction layer of about 100 µm. In Fig. 3, the SEM micrograph of the cross-section of the $Al_{46}Ti_{46}Ta_8$/YSZ sample is shown.

Since both alloys showed strong interactions with the selected candidate refractory materials, the additional tests were done with ceramics whose surface was covered with

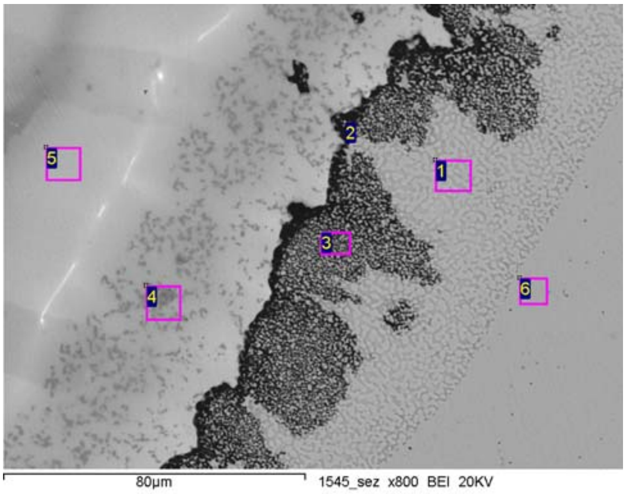

	O [at%]	Al [at%]	Ti [at%]	Y [at%]	Zr [at%]	Ta [at%]	W [at%]
1	55.75	12.79	11.51	2.53	15.61	1.81	
2	71.64	26.22	0.23	1.91			
3	74.14	17.74	0.48	1.28	6.35		
4	46.19	23.39	17.77	8.41	0.72	2.95	0.57
5		43.26	45.92			10.05	0.77
6	76.79			1.83	21.38		

Fig. 3 SEM micrograph and EDS analysis (at%) of $Al_{46}Ti_{46}Ta_8$ alloy/Zirconia interface after the wetting experiment

protection coating by deposition of Y_2O_3 spray followed by thermal treatment, as described above.

Covering with Y_2O_3 spray was found to reduce the interaction of $Al_{46}Ti_{46}X_8$ alloys with alumina, both SC and PC, showing non-wetting ($\theta > 90°$). However, after longer contact time (>1 min), the Y_2O_3-based protective layer on sapphire surface tends to be detached. In particular, fragmentation and introduction of its separated parts into the liquid alloy, partial covering of the drop surface occurred and, thus, making this procedure inappropriate for the surface tension measurements. On the contrary, the same Y_2O_3-based layer on a flat polycrystalline alumina substrates polished up to ~150–200 nm roughness exhibits acceptable stability. Therefore, this type of substrate coated by a Y_2O_3-based layer was selected for surface tension measurement by the pendant/sessile drop combined method.

Surface tension results

Oscillating drop

The surface tension measurements of the $Al_{46}Ti_{46}Nb_8$ and $Al_{46}Ti_{46}Ta_8$ alloys by oscillating drop method were performed in the temperature ranges of $T = 1613 \div 1947$ K and $1725 \div 1894$ K, respectively. Figure 4 shows the measured surface tension of both liquid AlTi-based ternary alloys. The temperature dependences are described by the following linear equations:

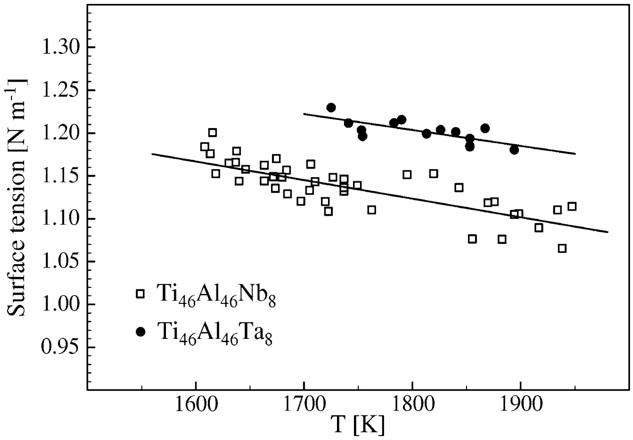

Fig. 4 Surface tension of liquid $Al_{46}Ti_{46}Nb_8$ (*open square*) and $Al_{46}Ti_{46}Ta_8$ (*filled circle*) as a function of the temperature measured by oscillating drop method (The lines are linear fits to the data)

$$\gamma_{TiAlNb} = 1.114 \pm 0.05 - (2.17 \pm 0.3) \cdot 10^{-4} \cdot (T - 1842) \quad [\mathrm{N\,m^{-1}}] \qquad (3)$$

$$\gamma_{TiAlTa} = 1.19 \pm 0.09 - (1.9 \pm 0.5) \cdot 10^{-4} \cdot (T - 1890) \quad [\mathrm{N\,m^{-1}}] \qquad (4)$$

Pendant and sessile drop

Surface tension measurements by the pendant/sessile drop combined method as described above have been performed under an atmosphere of a flowing pure Argon (99.9999%, $[O_2] < 0.1$ ppm; ArN60-Air Liquide) and at the temperature values of $T = 2007$ K and $T = 2063$ K for $Al_{46}Ti_{46}Nb_8$ and $Al_{46}Ti_{46}Ta_8$, respectively. In order to obtain freshly formed alloy drop for surface tension measurements under oxide-free conditions, the alloys have been squeezed from alumina capillary immediately after alloy melting. The overheating up to 2007 K and up to 2063 K of the $Al_{46}Ti_{46}Nb_8$ and $Al_{46}Ti_{46}Ta_8$, respectively, was needed making possible the squeezing through the small hole of the capillary. Owing to good wetting with dense alumina, problems with the detachment of the droplets from the alumina capillary can occur. Thus, in order to avoid 'a flooding' by the liquid alloys, the droplets have been deposited on the Y_2O_3-treated alumina substrate by the procedure described above. In the case of $Al_{46}Ti_{46}Ta_8$ alloy, a further heating (up to 2089 K) was needed for the detachment and the formation of the sessile droplet on the plate. As an example, the time evolution in the formation of the $Al_{46}Ti_{46}Nb_8$ alloy drop during surface tension experiment is shown in Fig. 5.

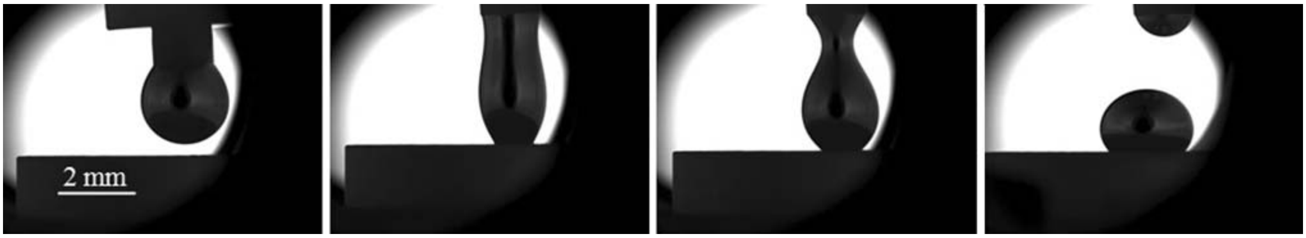

Fig. 5 Time evolution in the formation of the $Al_{46}Ti_{46}Nb_8$ alloy drop during surface tension experiments by combined pendant drop/sessile drop method

Table 1 Surface tension data of $Al_{46}Ti_{46}Nb_8$ and $Al_{46}Ti_{46}Ta_8$ (at $T = 2007$ K and $T = 2063$ K, respectively) obtained by pendant drop, sessile drop and oscillating drop methods

Method	$Al_{46}Ti_{46}Nb_8$ at $T = 2007$ K		$Al_{46}Ti_{46}Ta_8$ at $T = 2063$ K	
	γ (*N/m*)	St. Dev.	γ (*N/m*)	St. Dev.
Pendant drop	1.106	0.007	1.150	0.015
Sessile drop	1.072	0.023	1.105[a]	–
Oscillating drop	1.078	0.05	1.157	0.09

[a] The surface tension value of $Al_{46}Ti_{46}Ta_8$ sessile drop has been obtained at $T = 2089$ K

The elaboration of the images acquired each 0.1 s^{-1} during the surface tension measurements allowed the surface tension data obtained by both the pendant drop and the sessile drop. Table 1 shows the values of the surface tension of $Al_{46}Ti_{46}Nb_8$ and $Al_{46}Ti_{46}Ta_8$ at $T = 2007$ K and $T = 2063$ K, respectively, measured by the three different methods, e.g. sessile drop, pendant drop and oscillating drop methods. For both alloys, the surface tension values obtained by the pendant and the sessile drop are consistent for each other, and a good agreement exists also with the corresponding experimental values obtained by the oscillating drop method at the same temperature.

Modelling of the surface tension of liquid Al–Ti–Nb and Al–Ti–Ta ternary alloys

Theoretical background

Butler's equation has been extensively used to calculate the surface tension of binary and multicomponent alloy systems [15]. All theoretical models such as the regular solution model, the sub-regular solution model, the compound formation model, the self-aggregating model, etc. are based on Butler's equation, but the equation parameters related to the thermodynamic quantities or structural data are described using different expressions [16–21].

On the basis of Butler's equation, the surface tension of liquid alloys assuming the regular solution model can be calculated by

$$\sigma = \sigma_i + \frac{RT}{S_i}\ln\frac{X_i^s}{X_i^b} + \frac{1}{S_i}[G_i^{xs,s}(T, X^s_{j(j=2,3)}) - G_i^{xs,b}(T, X^b_{j(j=2,3)})], i = 1,2,3. \tag{5}$$

where R, T, σ_i and S_i are gas constant, temperature, surface tension of pure components and surface area, respectively. The surface area of component i is calculated from the Avogadro's number, the atomic mass and the density data, as

$$S_i = 1.091 N_0 \left(\frac{M_i}{\rho_i}\right)^{2/3} \tag{6}$$

$G_i^{xs,s}(T, X^s_{j(j=2,3)})$ and $G_i^{xs,b}(T, X^b_{j(j=2,3)})$ are partial excess Gibbs energies of i in the surface phase as a function of T and $X^s_{j(j=2,3)}$ and that of i in the bulk phase as a function of T and $X^b_{j(j=2,3)}$. The excess energy term of a component i can be derived from the standard thermodynamic relation, in the form

$$G_i^{xs} = G^{xs} + \sum_{j=1}^{n}(\delta_{ij} - X_j)\frac{\partial G^{xs}}{\partial X_j} \tag{7}$$

where δ_{ij} is Kronecker's symbol, and

$$G_i^{xs,s}(T, X^s_{j(j=2,3)}) = \beta G_i^{xs,b}(T, X^b_{j(j=2,3)}) \tag{8}$$

β is a parameter describing the reduced coordination in the liquid phase.

Calculated surface tension of liquid Al–Ti–Nb and Al–Ti–Ta ternary alloys

In order to predict more precisely the surface tension of liquid Al–Ti–Nb and Al–Ti–Ta ternary alloys, the Butler's model has been applied. The excess Gibbs energy terms of the Al–Nb, Al–Ta, Ti–Nb and Ti–Ta liquid phases were taken from [22], whilst the liquid phase of Al–Ti was described by [23]. The data on the melting temperatures, densities and molar volumes were taken from [24], whilst the surface tension reference data of liquid Al [25], Ti, Nb [26] and Ta [27] were obtained by different experimental methods and, accordingly, was not possible to estimate correctly an overall error of the calculated surface tension values.

Considering the phase diagrams of the aforementioned binary subsystems at temperatures close to 1973 K, it is important to mention that with an exception of the Al–Ti, all the other systems exhibit the presence of solid phases over wide composition intervals. Accordingly, the surface tension of liquid Al–Ti–X (X = Nb, Ta) alloys has been calculated at $T = 2073$ K by Butler's model in the regular solution approximation (Eq. 5) combining the corresponding thermodynamic data on the Gibbs excess free energy of binary Al–Ti, Al–Nb and Nb–Ti as well as Al–Ta and Ti–Ta systems.

Taking into account the phase diagrams of the binary subsystems corresponding to the ternary Al–Ti–Nb system at 2073 K, the Nb-rich part of the Al–Nb and 80% of the Nb–Ti systems represent the solid phases, and thus, some data were obtained considering the significant degree of undercooling. The situation is still worse in the case of the Al–Ti–Ta system, for which the corresponding phase diagrams of its binary subsystems indicate the presence of solid phases in a wider part of Ta-rich of the Al–Ta and 90% of the Ta–Ti systems, which contribute to a higher degree of undercooling.

In order to establish the effects of the third component, Nb, on the experimental surface tension values of ternary alloys, the experimental data obtained by different methods have been compared with corresponding binary Al–Ti alloys with the same Ti content. Taking into account the thermodynamic experimental data of liquid Al–Ti alloys obtained at 2000 K [22], the calculations of their surface tension isotherms were performed at $T = 1973$ K. The surface tension experimental data of the $Al_{46}Ti_{46}Nb_8$ alloy obtained by different experimental techniques exhibit a good agreement (Fig. 6). The presence of Nb significantly increases the surface tension of ternary alloys.

The variations of the surface tension of the Al–Ti–Nb alloys with composition, in terms of the iso-surface tension lines, have been calculated by the regular solution model at $T = 2073$ K (Fig. 7). When compared, the experimental value of the surface tension of the $Al_{46}Ti_{46}Nb_8$ alloy measured by using the EML-OD technique was $\gamma = 1.064$ N m^{-1}, which differs about 11% from the corresponding value predicted by Butler's equation, $\gamma = 1.0$ N m^{-1}, as indicated by square symbol inside the Gibb's triangle shown in Fig. 7. As can be expected, the experimental data obtained at 2007 K by the SD and PD techniques exhibit slightly higher difference with respect to the calculated one.

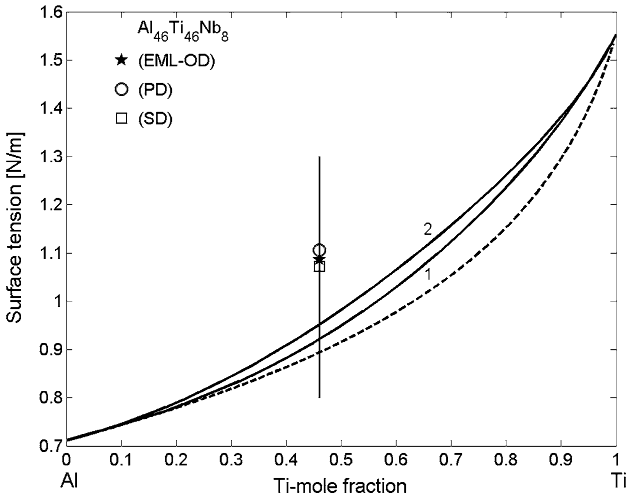

Fig. 6 Surface tension of liquid $Al_{46}Ti_{46}Nb_8$ alloy obtained by different experimental techniques: EML-OD, SD and PD. For a comparison, the Al–Ti isotherms (1: Regular solution; 2: Compound Formation Model) calculated at 1973 K are shown

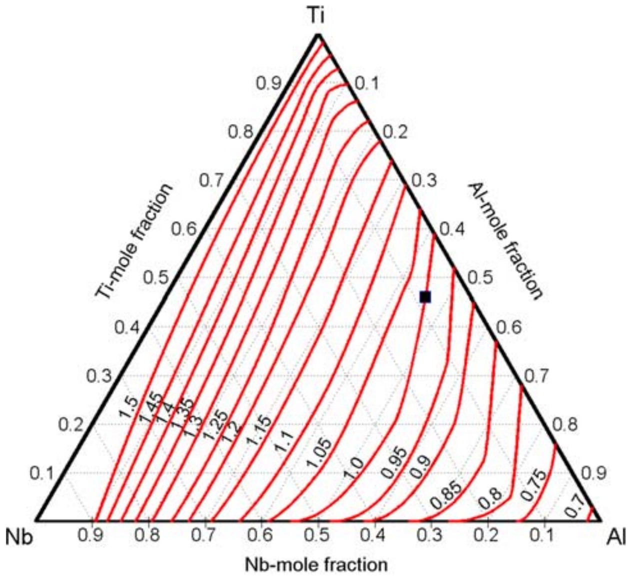

Fig. 7 Iso-surface tension lines of liquid Al–Ti–Nb alloys calculated by the Butler's equation for the regular solution model at 2073 K. The square symbol (*filled square*) represents the composition location of the $Al_{46}Ti_{46}Nb_8$ (at%) in the Gibbs triangle and the corresponding surface tension calculated value ($\gamma = 1.0$ N m^{-1})

Similarly, the effects of Ta on the experimental surface tension values of ternary $Al_{46}Ti_{46}Ta_8$ alloys have been analyzed by comparing the experimental data obtained by different methods with corresponding binary Al–Ti alloys with the same Ti content. The presence of Ta significantly increases the surface tension of ternary alloys (Fig. 8).

The experimental data obtained at $T = 2089$ and $T = 2063$ K, using SD and PD, respectively, exhibit, in

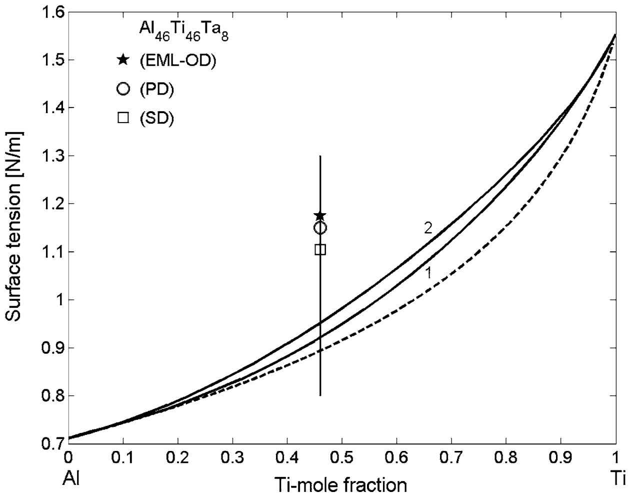

Fig. 8 Surface tension of liquid $Al_{46}Ti_{46}Ta_8$ alloy obtained by different experimental techniques: EML-OD, SD and PD. For a comparison, the Al–Ti isotherms (1: Regular solution; 2: Compound Formation Model) calculated at 1973 K are shown

particular for the data from the PD measurements, a good agreement with those obtained by the EML-OD experiments as well as with the corresponding predicted values. In order to analyse the surface tension variations with composition, the iso-surface tension lines of the Al–Ti–Ta alloys have been calculated by the regular solution model at $T = 2073$ K (Fig. 9).

The bigger difference between the experimental (EML-OD) and theoretical surface tension values, $\gamma = 1.156$ N $m^{-1}$and $\gamma = 1.0$ N m^{-1}, respectively, observed in the case of the $Al_{46}Ti_{46}Ta_8$ alloy, can be attributed to a high uncertainty of Ta surface tension data [27] with respect to that of Nb [26], taken as the reference data in the present calculations.

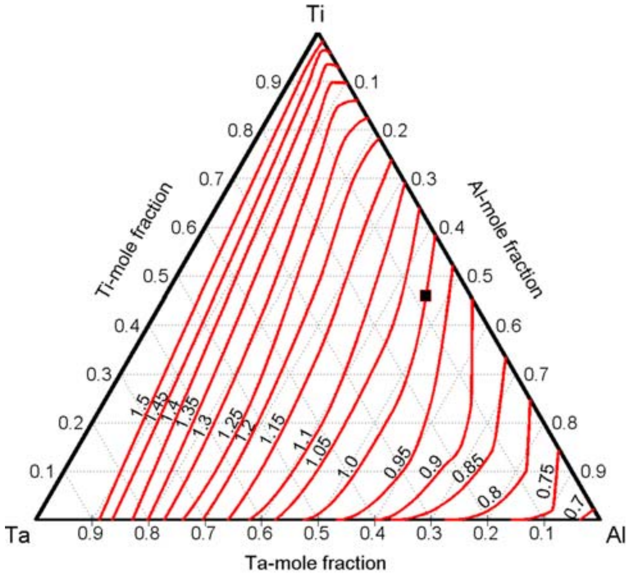

Fig. 9 Iso-surface tension lines of liquid Al–Ti–Ta alloys calculated by the Butler's equation for the regular solution model at 2073 K. The square symbol (*filled square*) represents the composition location of the $Al_{46}Ti_{46}Ta_8$ (at%) in the Gibbs triangle and the corresponding surface tension calculated value ($\gamma = 1.0$ N m^{-1})

In both cases, the presence of Nb and Ta significantly increases the surface tension of TiAl-based ternary alloys. On the contrary, it is well known that the presence of the short range order phenomena in the liquid phase may increase the surface tension of melts. Although the structural experimental data on these ternary alloys are lacking, the presence of the short range order phenomena in their binary sub-systems may indicate similar effects of these phenomena on the surface tension of Al–Ti–Nb and Al–Ti–Ta alloys.

Conclusions

The surface tension of two ternary γ-TiAl-based alloys, namely the $Al_{45.5}Ti_{46.5}Nb_8$ and $Al_{45.5}Ti_{46.5}Ta_8$, have been determined. The measurements have been performed in parallel by different laboratories, applying the container-less oscillating droplet method by the electromagnetic levitation and a combined method using two methodologies in one test (i.e. the pendant drop and sessile drop) by an advanced experimental complex that has been designed for investigations of high temperature capillarity phenomena. The container-less method allowed measuring the surface tension of the two ternary alloys in a wide temperature range including an undercooling regime.

Before the application of the new combined aforementioned method, preliminary interaction tests between the alloys investigated and different ceramic substrates have been performed with the aim to find the most suitable crucible material and, thus, to address correctly surface tension measurements. These tests have shown high reactivity of both alloys with all selected ceramics, even with the novel polycrystalline ZrO_2 substrates produced by high-temperature sintering using addition of Y_2O_3 nanoparticles that were found recently to be effective for reduction of the reactivity of Ni- and Ti-based alloys.

In order to obtain reliable surface tension experimental data, preliminary tests have been performed before the measurements. Taking into account the kinetic factors playing dominant role in the interactions between the $Al_{45.5}Ti_{46.5}X_8$ (X = Nb, Ta) melts and a ceramic substrate, different ceramics have been tested. All the tests were made under the same experimental conditions, looking for a chemically resistant material at least for a short time, at the beginning of testing, in the way that the reactivity at a melt/substrate interface is negligible.

It has been demonstrated that for the pendant drop method, such conditions can be achieved by reduction of alloy/ceramic true contact through the presence of native primary oxide film on the $Al_{45.5}Ti_{46.5}X_8$ alloys during their melting in alumina capillary. For the next step, sessile drop test of oxide-free droplets produced by squeezing the alloy through capillary, the yttria-based porous barrier layer on alumina substrate has found to have satisfactory stability.

These measurements combined with the pendant drop method have been performed under an atmosphere of flowing pure Argon at the temperatures of $T = 2007$ K and $T = 2063$ K, for the $Al_{45.5}Ti_{46.5}Nb_8$ and $Al_{45.5}Ti_{46.5}Ta_8$, respectively. The comparison between the surface tension values obtained by the three different methods showed a good agreement, encouraging further applications of this experimental approach to measure highly reactive metal systems and for investigation of oxidizable alloys.

In addition, the surface tension experimental results have been analysed from two points of view. The first one was aimed to estimate the effects of the third component, Nb or Ta, on the surface tension of the Al–Ti system, comparing the ternary experimental data with the calculated surface tension isotherms of liquid Al–Ti alloys having the same Ti-content, whilst the second one gives an insight into the variations of the surface tension with composition for both ternary alloy systems, the Al–Ti–Nb and Al–Ti–Ta. For this purpose, to calculate the iso-surface tension lines of liquid ternary alloys, Butler's model in the regular solution approximation combined with the corresponding thermodynamic data on mixing of binary subsystems has been applied. In both cases, the presence of Nb and Ta significantly increases the surface tension of TiAl-based ternary alloys. On the contrary, the presence of the short range order phenomena in the liquid phase may increase the surface tension of melts. Although the structural experimental data on the ternary alloys investigated are lacking, the presence of the short-range order phenomena in their binary sub-systems may indicate similar effects of these phenomena on the surface tension of Al–Ti–Nb and Al–Ti–Ta alloys and can justify the discrepancy between the calculated and the experimental values.

Finally, as general conclusion, the obtained surface tension data yield a further characterization of this technologically relevant class of alloys for which the literature data are lacking. In addition, following one main objective of the IMPRESS project, they can be addressed to be used as reliable experimental input data for the casting process simulation models.

Acknowledgements This study has been partially supported by the European Union (6th E.C. Framework Programme) in the framework of the IP IMPRESS (Contract NMP3-CT-2004-500635) financed research project. Financial support from the Foundry Research Institute has also been acknowledged.

References

1. Lapin J, Pelechova T, Domankova M, Daloz D, Nazmy M (2007) Metall Mater 45:121
2. Jarvis DJ, Voss D (2005) Mater Sci Eng A 413–414:583
3. Kuang JP, Harding RA, Campbell J (2001) Int J Cast Met Res 13:277
4. Johnson DR, Masuda Y, Inui H, Yamaguchi M (1997) Acta Mater 45:2523
5. Egry I, Brooks R, Holland-Moritz D, Novakovic R, Matsushita T, Ricci E, Seetharaman S, Wunderlich R, Jarvis D (2007) Int J Thermophys 28:1026
6. Choudhury NS, Graham HC, Hinze JW (1976) In: Foroulis ZA, Pettit FS (eds) Properties of high temperature alloys. The Electrochemical Society, Princeton, p 668
7. Lang C, Schütze M (1997) Mater Corros 48:13
8. Herlach DM, Cochrane RF, Egry I, Fecht HJ, Greer AL (1993) Int Mater Rev 38:273
9. Fabrichnaya O, Seifert HJ, Ludwig T, Aldinger F, Navrotsky A (2001) Scand J Metall 30:17
10. Barzilai S, Aizenshtein M, Froumin N, Frage N (2006) J Mater Sci 41:5108. doi:10.1007/s10853-006-0435-7
11. Cummings DL, Blackburn DA (1991) J Fluid Mech 224:395
12. Naidich YuV (1981) In: Cadenhead DA, Danielli JF (eds) Progress in surface and membrane science, vol 14. Academic Press, New York
13. Sobczak N, Nowak R, Radziwill W, Budzioch J, Glenz A (2008) Mater Sci Eng A 495:43
14. Garandet JP, Vinet B, Gros P (1994) J Colloid Interface Sci 165:351
15. Butler JAV (1932) Proc R Soc A135:348
16. Singh RN (1987) Can J Phys 65:309
17. Singh RN, Sommer F (1997) Rep Prog Phys 60:57
18. Speiser R, Poirier DR, Yeum K (1987) Scripta Metall 21:687
19. Tanaka T, Hack K, Hara S (1999) MRS Bull April 1999:45
20. Egry I, Brillo J, Matsushita T (2005) Mater Sci Eng A 413–414:460
21. Novakovic R, Ricci E, Giuranno D, Passerone A (2005) Surf Sci 576(1–3):175
22. Saunders N (1998) In: Ansara I, Dinsdale AT, Rand MH (eds) COST 507—Thermochemical database for light metal alloys, vol 2. European Communities, Luxembourg, p 89
23. Witusiewicz VT, Bondar AA, Hecht U, Rex S, Velikanova TYa (2008) J Alloys Compd 465:64
24. Iida T, Guthrie RIL (1993) The physical properties of liquid metals. Clarendon Press, Oxford
25. Lang G, Laty P, Joud JC, Desré P (1977) Z Metallkd 68(2):113
26. Ishikawa T, Paradis PF, Itami T, Yoda S (2003) J Chem Phys 118(17):7912
27. Vinet B, Magnusson L, Fredriksson H, Desré PJ (2002) J Colloid Interface Sci 255:363